TACTILE DISCRIMINATION OF SHAPE: RESPONSES OF SLOWLY ADAPTING MECHANORECEPTIVE AFFERENTS TO A STEP STROKED ACROSS THE MONKEY FINGERPAD

ROBERT H. LAMOTTE AND MANDAYAM A. SRINIVASAN

Made in United States of America
Reprinted from THE JOURNAL OF NEUROSCIENCE
Vol. 7, No. 6, June 1987

The Journal of Neuroscience, June 1987, 7(6): 1655–1671

Tactile Discrimination of Shape: Responses of Slowly Adapting Mechanoreceptive Afferents to a Step Stroked Across the Monkey Fingerpad

Robert H. LaMotte and Mandayam A. Srinivasan

Department of Anesthesiology, Yale University School of Medicine, New Haven, Connecticut 06510

The representation of shape in the responses of slowly adapting mechanoreceptive afferent fibers (SAs) in monkeys was investigated. A series of flat plates was used, each having an increase in thickness (a step) in the middle so that one-half of the plate was thicker than the other. The cross-sectional shape of the step approximated that of a half-cycle of a sinusoid. The height of the step was fixed at 0.5 mm, while its width (half-cycle wavelength) was varied from 0 to 3.13 mm, resulting in step shapes that varied in steepness and curvature. The steps fell into 2 categories, characterized as "steep" and "gradual." A servocontrolled mechanical stimulator stroked each step across the distal fingerpad from the high to the low side of the step and back, while maintaining the contact force at 20 gm wt. Evoked action potentials in single SAs innervating the fingerpads of anesthetized monkeys were recorded.

Each SA's response to a step provided a spatial response profile (discharge rate as a function of step position) that reflected the distribution of curvature across the step shape. All the major features of the SA response could be consistently explained as being due to the sensitivity of the SA to the amount and rate of change in skin curvature. The response profile was altered by changes in stroke direction, step shape, and stroke velocity. Differences in stroke direction (back and forth) were indicated by (1) differences in pattern of response: a "burst-pause-burst" for strokes from high to low, and a "pause-burst-pause" for strokes from low to high; (2) a greater discharge rate in response to the step for low to high strokes, and (3) for some SAs, the reduction or absence of basal discharge in one of the directions. The discharge rate during the burst for either direction of stroking was greater for steep than for gradual steps, and increased, for a given step shape, with increases in stroke velocity. Regardless of differences in stroke velocity, steep steps were distinguished from gradual steps by having narrower burst widths for low-to-high strokes and narrower pause widths for high-to-low strokes.

The same stimuli were delivered to the human fingerpad, and the capacities of humans to discriminate between the steps were measured. It was concluded that the spatial features of SA responses, representing the widths of regions of active and inactive SA populations, as well as the intensive feature of discharge rate, accounted for the gross sensory discriminations of shape. Further, it was hypothesized that finer sensory discriminations of shape were based on differences in the discharge rate evoked in both the SA and the rapidly adapting mechanoreceptive fiber populations.

When exploring the surface of an object with the hand, the distal fingerpads are of prime importance for the tactile recognition of local variations of surface contour. The density of mechanoreceptors in the hand is greatest on the distal volar fingertip, or fingerpad, where tactile spatial resolution is also the best (Johansson and Vallbo, 1979; Darian-Smith and Kenins, 1980). Discrimination between shapes of sizes larger than the area of contact between the fingerpad and the object (about 7–12 mm diameter in humans) requires multiple contacts and thus may involve an integration of cutaneous and proprioceptive information with the knowledge of intended movements. However, certain shapes small enough to be within the contact area can be perceived with information solely from tactile receptors. Such small shapes were used in the present and 2 companion papers (LaMotte and Srinivasan, 1987; Srinivasan and LaMotte, 1987) in the study of how shape is encoded in the neural discharges of cutaneous mechanoreceptive afferents innervating the monkey fingerpad. These neural events were then compared with the human capacity to make tactile discriminations of shape. One question considered throughout these studies was the following: Given the geometrical properties of the shape of an object and the manner in which the object comes in contact with the skin, what is the relationship between these properties of shape, the spatial profile of skin deflection, and the resulting pattern of discharge in mechanoreceptors? Once this relationship is known, it should be possible to predict how any shape applied in a given manner is represented in mechanoreceptor responses.

What are the features of shape that might be represented in mechanoreceptor discharge? The most important is surface curvature, since the shape of a 3-dimensional object is completely described by the distribution of curvatures on its surface. The curvature at a point on a surface, as viewed in profile, is defined as the reciprocal of the radius of the circle that can be fitted to the surface locally at that point. The curvature distribution, or

Received June 16, 1986; revised Nov. 19, 1986; accepted Jan. 8, 1987

We thank Roland Johansson (University of Umea) for valuable input during the formative stage of the study and for calculating the parameters for the construction of half-cycle sinusoids. We also thank David Reddy and David Stagg for computer programming, James Whitehouse for his assistance in all phases of the study, and Linda Shiffrin for typing the manuscript. This research was supported by PHS Grant 15888.

Correspondence should be addressed to Robert H. LaMotte, Ph.D., Department of Anesthesiology, Yale University School of Medicine, 333 Cedar Street, New Haven, CT 06510.

shape, is invariant with respect to changes in the position and orientation of the object.

The contact of an object with the skin produces a spatial distribution of skin displacements that is directly related to the shape of the object. The pattern and rate of skin displacement differ according to how contact is made; for example, whether the fingerpad is simply pressed against the object and held still, or whether the finger moves across the surface of the object. Cutaneous mechanoreceptors have been classified according to how they respond to steady versus time-varying vertical indentations produced by punctate probes (e.g., Talbot et al., 1968; Johansson and Vallbo, 1979; Pubols and Pubols, 1983), but not to surfaces that vary in shape. Recently, the responses of mechanoreceptive afferents to spatial patterns that were moved across or vertically applied to the fingerpad of the monkey were investigated (Darian-Smith and Oke, 1980; Darian-Smith et al., 1980; Johnson and Lamb, 1981; Phillips and Johnson, 1981a; Lamb, 1983). However, the spatial parameters that were varied were the sizes and spacings of raised elements (dots, bars) and not the shapes of the elements. Thus, there is little information on how shape is represented in the responses of cutaneous primary afferents.

In order to study the sensitivity of cutaneous mechanoreceptors to changes in shape, we employed a series of flat plates, each having an increase in thickness (a step) in the middle so that half of the plate was thicker than the other. The cross-sectional shape of the step approximated that of a half-cycle of a sinusoid. The height of the sinusoidal step was fixed at 0.5 mm, while its width (half-cycle wavelength) was varied from 0 to 3.13 mm, which resulted in step shapes that varied in steepness and curvature. Thus, the step shapes were characterized as having the same curvature profile (i.e., sinusoidal), with each having a different peak curvature and wavelength.

Each step was applied under machine control to the passive fingerpad. In the first 2 papers of the present series, the responses of mechanoreceptive afferents to steps stroked under constant compressional force across the monkey fingerpad are described: those of slowly adapting fibers (SAs) in the present paper and, in the following paper (LaMotte and Srinivasan, 1987), the responses of Meissner corpuscle, rapidly adapting fibers (RAs). The machine-controlled step stroking was intended to reproduce the natural stimulus events generated when the finger is actively stroked across a stationary surface. In the third paper (Srinivasan and LaMotte, 1987) we describe responses of both fiber types to steps applied vertically and stepped, not stroked, across the fingerpad. Although this type of stimulus is less natural, it is simpler since each point on the skin surface within the contact area moves synchronously. A further advantage is that the roles of RAs and SAs in encoding shape can be separated, since only the SAs respond during the steady phase of the stimulation.

The results described in these 3 papers suggest that human tactile discrimination of the shapes used is based upon 2 sets of cues—one that is intensive (step sharpness or peak curvature), the other spatial (step width or wavelength). Under stroking, better intensive information is provided by RAs, while superior spatial information is given by SAs. Under vertical indentation (without stroking), SAs are superior in providing both spatial and intensive information. Under either stroking or indentation, SAs, and not RAs, provide direct information about the curvature profile of the step shape. Models of mechanoreceptor responses that could relate the discharges of SAs and RAs to observable events on the skin are proposed. The responses of RAs are predominantly influenced by the vertical velocity of the skin, while SAs are highly sensitive to changes in the curvature of the skin surface.

Materials and Methods

Shapes of the steps. Each step was made of a transparent epoxy plate (20 × 45 mm) containing a transition in height between 2 planes. The shape of the transition was varied and, in longitudinal cross section, approximated a half-cycle of a sinusoid. These shapes were originally cut in soft D2 tool steel by a computer-controlled wire electric discharge machine (Shape Cut Corp., Torrington, CT). The half-cycle was taken from the negative to the positive peak of the sine wave, i.e., from the beginning of curvature on the bottom or low side to the end of curvature at the top. The height of each step was fixed at 0.5 mm, while its "width" or the half-cycle wavelength was varied. The roughness of the cut metal surface was reduced by fine polishing with jeweler's rouge to achieve an R_a (roughness centerline average) of less than 1 μm. Then a mold of each step was made with silicone rubber. Clear epoxy was poured into these molds to produce transparent positive replicas of the original steps.

Profiles of each of the steps were measured by a contour-measuring device that traversed a stylus, with a radius of less than 0.25 mm, across the surface.[1] Profiles were measured along 3 parallel longitudinal paths. A profile of each step obtained from tracing the middle longitudinal path is shown in Figure 1. The steepest step was a sharp, 90° transition from the low to the high side and was not traced with the contour-measuring device. The beginning and end of the sinusoidal portion of each measured profile were estimated by eye. The closest-fitting sine wave to the upper half was determined by a least-squares procedure. The profiles were found to be acceptably represented by sine waves with small residual variances of less than 20 μm^2. The quarter-cycle measurements obtained from the 3 different traverses along each step were averaged and multiplied by 2 to obtain the half-cycle wavelength (Fig. 1), which differed because of track positions by at most 1%. The step widths, i.e., the half-cycle wavelengths of the steps, were 0.450, 1.195, 1.230, 3.038, and 3.134 mm. The steps were also numbered from 0 to 5 in the order of steepest to most gradual. Steps 0–3 were classified as "steep" and 4 and 5 as "gradual," based on the informal sensory judgments of human observers. The vertical dashed line in Figure 1 indicates the position of a reference line drawn on the back of each step marking the beginning of step curvature on the high side. As described below, these reference marks were used to spatially align the responses of a fiber to different steps to a fixed locus on the skin within the fiber's receptive field.

Applying the steps to the passive fingerpad. A servocontrolled hydraulic mechanical stimulator was used to displace the step along vertical and horizontal axes (Fig. 2; LaMotte et al., 1983). A given experimental run consisted of a series of trials. During each trial, 1 of 6 steps, arranged radially on a wheel (Fig. 2*B*), was selected by rotating the wheel with a stepping motor. The flat, high side of the step was brought vertically onto the skin (fingerpad) to achieve a desired compressional force. Maintaining this force, the step was first held stationary for 1 sec, then followed by a series of strokes with constant horizontal velocity back and forth across the skin (Fig. 2*A*). The step was then withdrawn from the skin and returned to the home position. The compressional force of the step against the skin and the horizontal and vertical displacements and velocities of the step were controlled with local analog feedback circuits preprogrammed before each stimulus presentation by a minicomputer (Northstar Horizon). The reactive force of the plate against the skin was measured with a force transducer (Sensotek) in contact with the top of the spring-loaded plate containing the step (Fig. 2*A*). The sequence of stimuli delivered and stimulus timing was also controlled by the minicomputer.

All stimuli were delivered to the volar surface of the distal phalanx of the finger. The hand was restrained in plasticine, with the finger to be stimulated held at a slightly higher level. The monkey finger was restrained by a plastic screw glued to the fingernail and was sunk into the plasticine. The human finger was restrained only by the plasticine. The sides of the fingerpad were not restrained, thereby allowing the fingerpad to move back and forth (without alteration in the position of the contact area on the skin) during lateral stroking, as it might if the fingertip were actively stroked over a passive surface. There was no

[1] We thank Theodore Vorburger and E. Clayton Teague of the U.S. National Bureau of Standards for making these measurements.

perceptible vibration or sticking of the step on the skin, and the stimuli felt natural to human subjects.

Consideration of the stimulus parameters to be controlled when stroking a step across the passive finger. Pilot experiments were carried out using controlled displacement, wherein the vertical position of the step (i.e., the plate attached to the step) was held constant during stroking. This resulted in an abnormally large change in force, sometimes of an order of magnitude, for movements from the low to high side of the step or vice versa. These sudden large changes were not observed when subjects actively touched a step, even though there was variation in overall contact force. Perhaps, during active touch, the stiffness of the finger joint was somehow set by the observer to passively follow the local variations in surface contour, thereby maintaining a more-or-less constant contact force. Thus, it was considered more natural to control the contact force than the vertical displacement of the plate to which the step was attached.

When force was held constant during machine-controlled stimulation of the passive finger, the depth of skin indentation was observed to be approximately constant. Subjects reported that each step appeared to move smoothly and "normally" across the finger, evoking sensations similar to those produced during active touch. There were no distracting vibrations or perturbations. Under lower stroke velocities of 10 mm/sec or less, the vertical displacement of the step clearly followed the shape of the step. However, at the higher stroke velocities, for example, 40 mm/sec, there was less compensation for force perturbations, and yet the sensations of the step's movements and shape were perceived as similar to those produced during active touch.

Contact forces generated during an active touch experiment. A pilot experiment was carried out to measure the contact forces generated on the fingerpad when the finger was moved over a step during tests of the human capacity to discriminate between steps 1 and 2. The subject's hand was comfortably restrained, while the middle finger was allowed to move in the mediolateral direction perpendicular to the long axis of the finger, so that the fingerpad was first brought into contact with the low side of the step and then stroked onto the high side. Only movements in the low-to-high direction were allowed during contact with the step. The region of contact between the skin and the step was recorded on videotape so that the range of forces could be determined for successive locations of the finger along the step. Each stroke began with initial contact with the low side of the step; contact force increased with the start of lateral movement, reaching a maximum as the finger approached the high side of the step, which was followed by further lateral movement and a decrease in force to 0 as the finger was withdrawn. Maximum contact forces ranged from 15 to 45 gm wt for 4 subjects and from 72 to 90 gm wt for another subject. All subjects were able to discriminate between steps 1 and 2 at a level exceeding 75% correct under the standard–standard versus standard–comparison forced-choice paradigm described below.

The results of these experiments indicated that contact force varied widely during active movements of the finger over a stationary step. It was also found that, when stroking steps by hand across the monkey's finger, variations in force affected the rate of discharge of SAs but not the spatial patterns. Thus, the choice of force for machine-controlled stimulation did not appear to be critical. Since humans could discriminate between steps with contact forces as low as 15 gm wt, and considering the smaller size of the monkey's finger, we chose a scaled-down contact force of 20 gm wt for most of the machine-controlled stimulations of the skin in the neurophysiological and psychophysical experiments.

Neurophysiological experiments. Action potentials were recorded from single mechanoreceptive afferent fibers in the upper or lower median nerves of 8 anesthetized juvenile *Macaca fascicularis* monkeys weighing 4–6 kg. The methods of electrophysiological recording, fiber dissection, and fiber classification have been previously described (e.g., Talbot et al., 1968). Only those fibers with receptive fields centered close to the center of the volar distal pad of the second, third or fourth finger were used. Mechanoreceptive afferents were classified as slowly adapting (SA) (as opposed to rapidly adapting, RA) if they exhibited a static discharge for more than 2 sec during a steady indentation of the skin by a 50 gm wt resting freely on the skin. All were of the Type I (SAI) and not the Type II (SAII) variety, as described for humans by Johansson and Vallbo (1979).

A dissection microscope equipped with a video camera allowed a 20× magnified view of the stimulated skin through the transparent step as the step was pressed onto and stroked across the skin (Fig. 2*A*). The

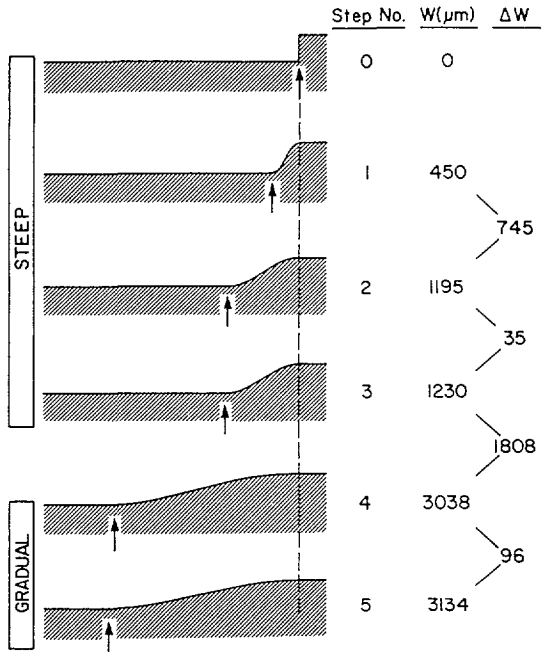

Figure 1. A cross-sectional profile of the shape of each step. The width of the step from the start of the convex curvature at the top of the step (*vertical dashed line* indicating the location of a reference mark) to the beginning of the flat portion at the bottom (*arrow*) is given in micrometers and is the half-cycle wavelength *W*. Differences in W (ΔW) between those steps used in studies of discrimination are also given. The height of each step is 0.5 mm. For convenience, the steps are labeled 0 to 5. Steps *0–3* are categorized as "steep" and steps *4* and *5* as "gradual."

output of the camera was viewed on a video monitor and recorded with a video cassette recorder. A video digital voltmeter placed between the camera and the video cassette recorder mixed the video input with (1) a numerically displayed voltage from the force transducer, (2) the cumulative number of action potentials from the start of a trial, (3) individual action potentials, each displayed when it occurred as a short horizontal line within a thin vertical strip at the left edge of the screen, (4) elapsed time in seconds from the start of the trial, and (5) the video field number, which continuously cycled from 0 to 59 during each second.

A PDP 11/34 computer collected analog signals at sampling intervals of 20 msec from transducers that indicated the vertical displacement of the step and the compressional force. The computer also collected digital information representing the time of occurrence of each action potential, the beginning of each video field, the start of each trial, and the start and end of each horizontal stroke of a step across the skin. The time to ramp up to or down from the desired horizontal velocity was 2–10 msec. Since both the computer and the video cassette recording contained a record of the cumulative field count during each trial, the occurrence of each action potential could be related to the location of the step on the skin.

Prior to the machine-controlled tactile stimulation, the receptive field of each fiber was mapped using von Frey monofilaments, each varying in stiffness and delivering forces ranging typically from 0.08 gm wt (0.13 mm diameter) to 1.9 gm wt (0.29 mm diameter). The papillary ridge pattern was drawn on an acetate sheet placed over the video monitor. In the monkey, the ridges run parallel to the long axis of the finger, except within several millimeters of the cuticle, where the ridges run perpendicular to this axis. Pen marks were superimposed on the drawing of ridges to indicate the skin location of each von Frey filament when one or more nerve impulses was evoked. Lines were drawn around the areas within which each of several different filaments evoked a response. After mapping the receptive field, a vertical line was drawn on the acetate sheet at a location approximately parallel to the ridges and near the edge of the receptive field, as obtained with the von Frey filament of medium stiffness. A thin black line on the top side of each step (marking the start of curvature from high to low sides of the step; Fig. 2*A*) was lined

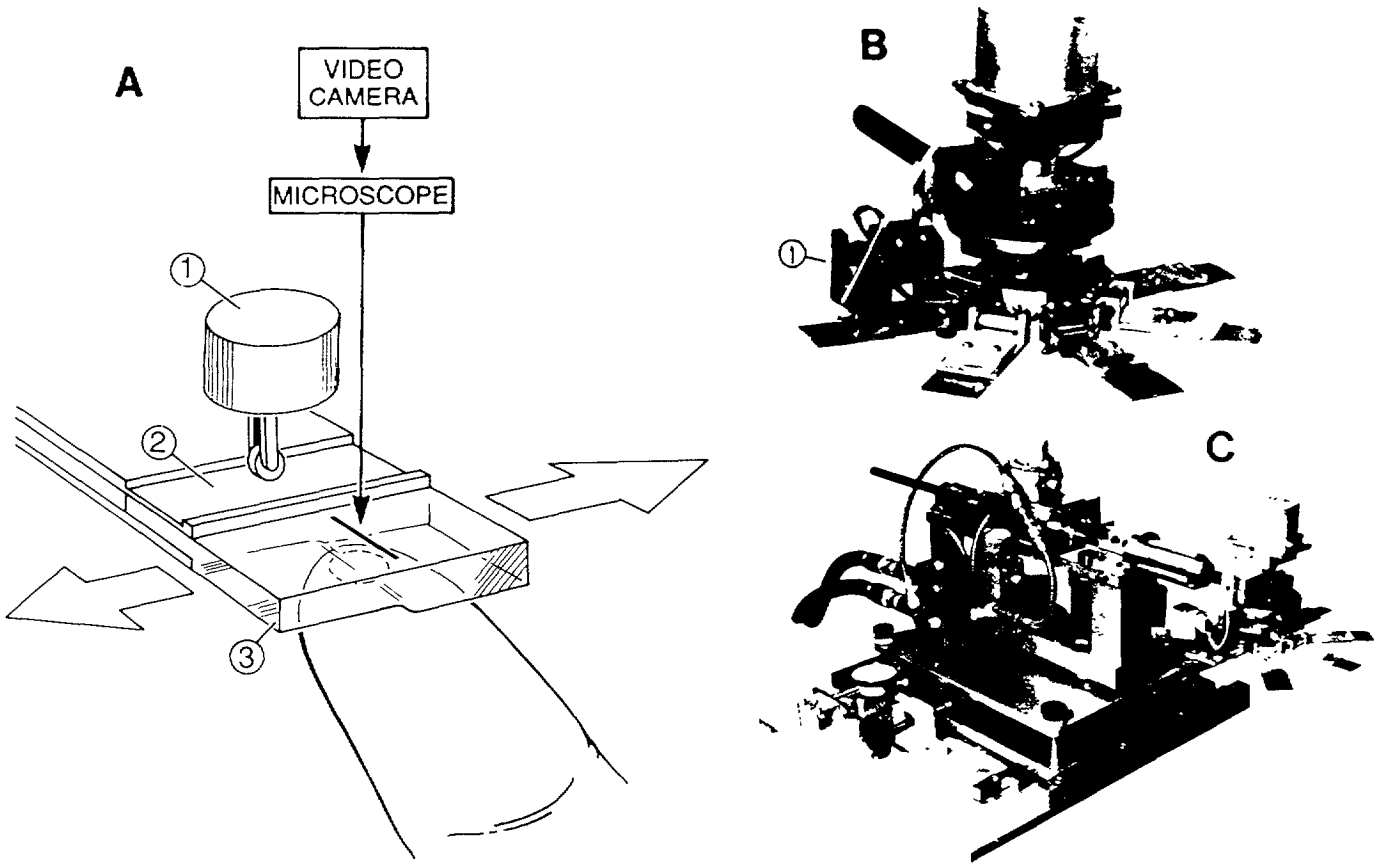

Figure 2. Illustrations of a step in contact with a finger and the tactile stimulator used to stroke the step across the fingerpad. *A,* Schematic drawing of the step when it is being stroked across the volar pad of the restrained finger. The step (*3*) is mounted to a spring-loaded plate (*2*) so that it exerts a base force against the force transducer (*1*) even when it is off the skin. The contact of the transparent step against the skin (*dotted oval*) is magnified through a microscope and recorded by means of a video camera and video cassette recorder. The *black line* on the top surface of the step is the reference mark (see text). *B,* Wheel used to change the steps. Different steps can be arranged radially on a wheel that, between trials, can be rotated by a stepping motor to bring the desired step into position under the force transducer (*1*). The step is then held in position by an electric brake. In this photograph, flat plates, not steps, are on the wheel. *C,* The entire tactile stimulator. The stepping-motor wheel assembly is attached to a shaft that can be moved up and down and horizontally (for stroking or stepping) by means of a servocontrolled hydraulic motor. The servo valves are under feedback control via displacement and force transducers and local control circuitry.

up with the reference line drawn on the acetate sheet by manually adjusting the tactile stimulator.

The spatial response profile of each fiber was obtained when each step was stroked over a distance of 18 mm, starting 9 mm to the left of the center of the most sensitive von Frey area. Prior to tests with each step, the horizontal start position for stroking was determined by lining up a cross-hair (located on the back of the step) with the receptive-field center. The cross-hair indicated a point on the high side of the step 9 mm away from the center of the sinusoidal portion of the step. The minicomputer recorded this position so that, on each trial, the plate was brought to this spot in the air before being lowered onto the skin. The skin was then vertically indented at 4 mm/sec until the desired force (20 gm wt) was obtained. The step remained stationary for 1 sec, followed by a horizontal displacement of 18 mm at a constant velocity from the high to the low side of the step while maintaining force, typically within ±2 gm wt. This was followed by a pause of 1 sec and a return stroke at the same force in the opposite direction, this time moving from the low to the high side of the step. After another pause of 1 sec, the process was repeated with another stroke back and forth, after which the step was lifted off the skin at a velocity of 4 mm/sec and returned in air to its home position, thus ending the trial. The time between each trial (i.e., between successive contacts with the finger) was approximately 6 sec. In some experiments, the stroke velocity was varied and 2 trials given at each of the following velocities: 1, 1.5, 5, 10, 20, and 40 mm/sec. In other experiments, 10 trials were given at a stroke velocity of 10 mm/sec, with 2 strokes in each direction per trial.

Psychophysical experiments on human subjects. We measured the sensory capacities of 5 naive humans to discriminate between different steps applied to the distal pad of the middle finger. Each subject's middle finger was elevated slightly above the rest of the hand and restrained in plasticine. In both of 2 series of tests, the steps were each stroked under machine control in one direction only, so that comparisons of discriminability could be made separately for the 2 directions of stroking. Each step was first brought down vertically, at a rate of 4 mm/sec, onto the finger on the low (or high) side of the step at the cross-hair (centered 9 mm from the center of the sinusoidal portion) until a force of 20 gm wt was reached. This force was then maintained during a pause of 1 sec, followed by a lateral stroke of 18 mm at 10 mm/sec to the other side of the step. After another pause of 1 sec, the plate was withdrawn from the skin at 4 mm/sec.

On each trial, 2 steps were presented in 2 possible sequences, S_1 and S_2. A "standard" was always presented first, followed either by the standard again (S_1) or a "comparison" (S_2). The subject was instructed to give either of 2 responses (R_1, R_2), i.e., to state whether the second step was the standard (R_1) or the comparison (R_2). The 2 stimulus sequences were randomized and presented with equal probabilities 24 times each for a given pair of steps. The step pairs of (1,2), (2,3), (3,4), and (4,5) were given. For 3 subjects, the steeper step was given as the

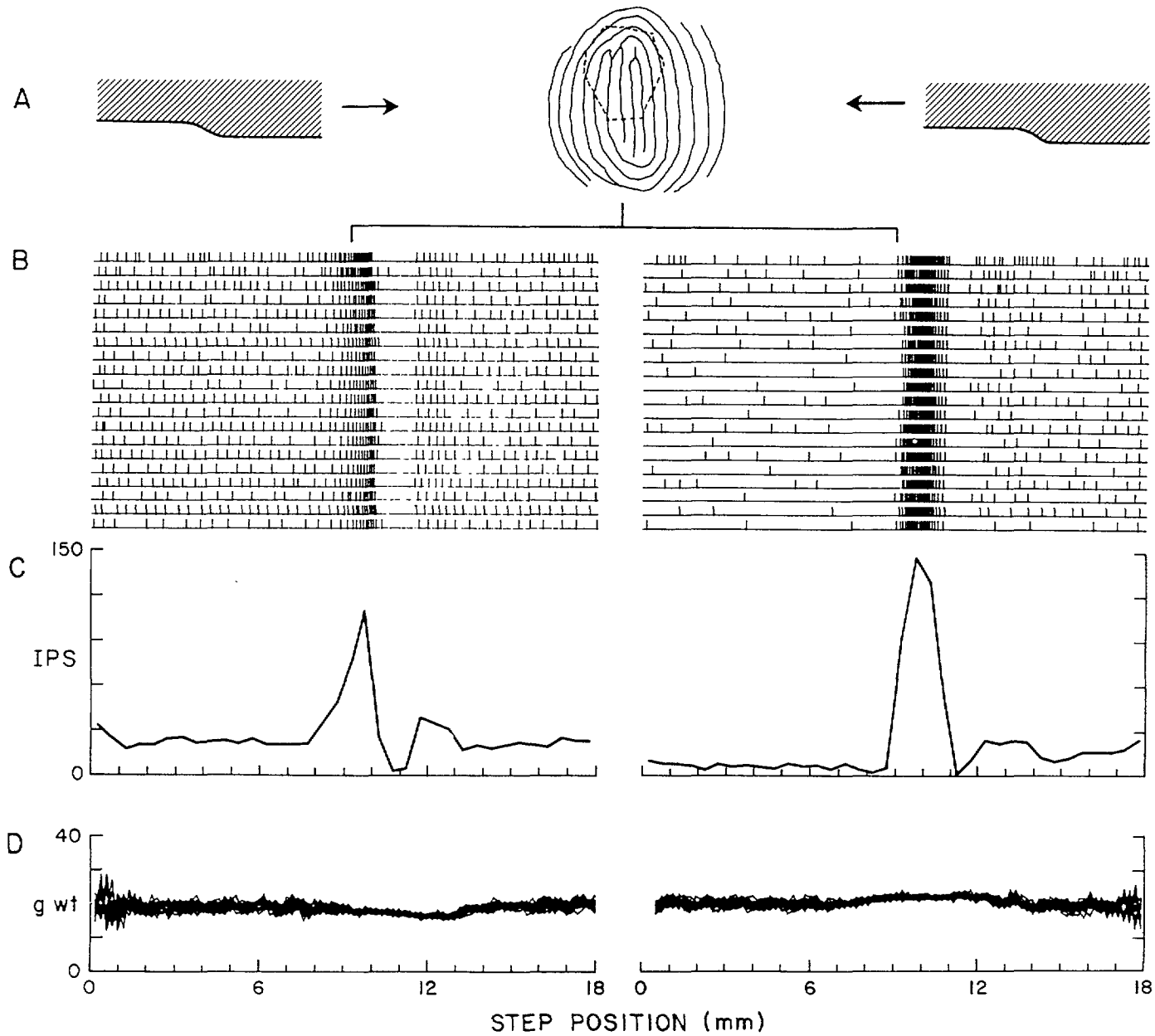

Figure 3. Responses of an SA (S26) to a step stroked across its receptive field. *A,* Schematic showing the cross-sectional profile of step 3, used to elicit the responses below. The sinusoidal portion of the step is drawn to scale but the total length of the step is less than actual. In the *middle* is a drawing of the papillary grooves on the monkey's fingerpad. The *dashed, oval line* indicates the boundary of the SA's receptive field, determined with a von Frey filament delivering a force of 0.17 gm wt. The scale is the same as that for the step positions during stroking, indicated below. On each trial, the step is stroked with a force of 20 gm wt at 10 mm/sec, first from left to right, i.e., from the high to the low side of the step, and then back again, going from low to high. *B,* Spatial plots of nerve impulses evoked in S26 during each stroke from left to right (*left panel*) and right to left (*right panel*). Each *vertical tic mark* indicates the spatial location of the reference mark (at the beginning of the convex curvature on the high side of the step) when an action potential occurred. On *each horizontal line* are the responses to a single stroke. Note that time begins at the left end for the left panel and at the right end for the right panel. The *branched line* connecting the papillary groove drawing to the spatial impulse plots indicates that point when the reference mark, and therefore the sharpest portion of the step, reached the center of the von Frey receptive field. *C,* Histograms of the mean discharge rate (impulses/sec or IPS) per consecutive bins of 0.5 mm, obtained from the data in *B. D,* Force applied by the step against the skin during each stroke in each direction. The force *traces* obtained from each of the 20 strokes in a given direction are superimposed.

standard, whereas for the other 2 subjects, the more gradual step was given as the standard. A bias-free measure of discrimination sensitivity, d', was calculated from the pairs of conditional probabilities, $p(R_1 | S_1)$ and $p(R_1 | S_2)$, which represented the proportion of trials in which the subject stated that S_1 occurred when, in fact, S_1 and S_2, respectively, were delivered (Johnson, 1980). For each of the 2 directions of stroking and for each subject, a psychometric function was constructed that plotted d' as a function of the difference in width (ΔW) between each pair of steps tested.

Statistical analyses. Repeated-measures analyses of variance were used to test the significance of the main effects of stroke direction, step shape, and stroke velocity on various measures of mean SA responses. Pairwise comparisons between individual means were made using the Newman-Keuls procedure (Winer, 1971). The significance level was set at 0.05.

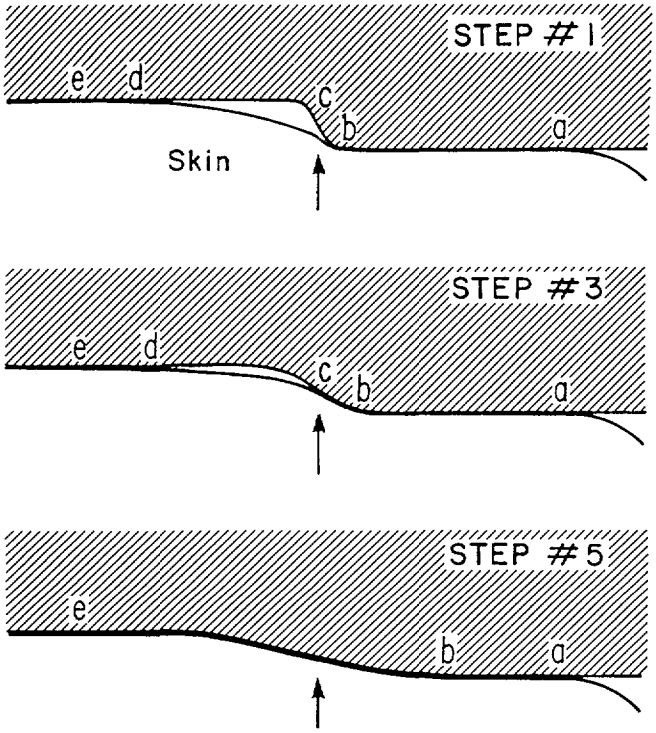

Figure 4. Schematized drawings of certain features of skin deflection produced by different steps when each is stroked across the fingerpad. Skin deflection profile is shown under each step (*1, 3,* and *5, shaded areas*). The letters *a* and *e* on each step mark the start (or stop) locations for stroking and are equidistant (9 mm) from the center of the step (shown by *arrows*). The sinusoidal portion of each step is drawn to scale but the lateral extent of the flat portions is shortened, and thus the numbered positions are not placed according to scale. The center of a fiber's receptive field can be visualized as located under *a* at the start of the strokes from left to right, i.e., from high to low sides of the step, and under *e* for strokes in the opposite direction. The locations *b, c,* and *d* refer to major events occurring during stroking (see main text). The stroke velocity was 10 mm/sec.

Results

General features of slowly adapting fibers to steps stroked across their receptive fields

Eight SAs were studied with machine-controlled stimulation. Each step was stroked back and forth, 20 times in each direction, along an 18 mm path. The stroke velocity was 10 mm/sec, and the contact force 20 gm wt. The responses of an SA (S26) to step 3 are shown in Figure 3. On each of 20 trials, the step was first stroked from the high to the low side (left column, Fig. 3) and then stroked back again from the low to high side (right column, Fig. 3). In Figure 3*B*, the instantaneous location of a reference mark (see Fig. 1) on the step is plotted at the occurrence of each nerve impulse. Beneath the impulse plots on each side of the figure is a histogram that averaged, over all 20 strokes, the discharge rate within consecutive distance bins of 0.5 mm (Fig. 3*C*). The point where the reference mark on the step reached the most sensitive spot within the von Frey map of the receptive field (Fig. 3*A*) is indicated by the branched line. Note that since the nerve impulses are plotted according to distance (step position) and not time, the strokes from low to high (right half, Fig. 3) start on the right and end on the left.

The characteristics of this SA's responses are representative of those observed for all of the 8 SAs tested. The frequency and pattern of responses to the step moving in a given direction were highly regular and reproducible, and reflected the distribution of curvature across the step profile. The major features of the response pattern could be directly related to the major features of the profile of skin deflection produced by the step. The side profiles of 3 different steps and a schematic drawing of the skin deflection profile under each step as it is being stroked under controlled force over the skin are shown in Figure 4. These drawings were based on videotape recordings while the skin was illuminated by means of a fiber-optic light positioned behind and to the side of the finger. The purpose of the schematic is to illustrate the sequence, during stroking, of stimulus events that might be expected to occur at the most sensitive spot on the skin surface within an SA's receptive field.

The major features of SA responses shown in Figure 3 can be interpreted in terms of the features of the skin deflection profile under step 3 as illustrated in Figure 4. The center of a fiber's receptive field can be visualized as being at position "a" in Figure 4 at the start of strokes from high to low, and at location "e" for low to high strokes. At the beginning of a stroke from high to low (left panels, Fig. 3), a short, transient response to skin stretch was generated, followed by a basal level of discharge in response to steady indentation by the flat portion of the step against the skin (locations "a–b," Fig. 4). When the curved (convex) portion of the step reached the most sensitive spot in the receptive field (vertical branched line, Fig. 3*A*), the discharge rate increased to a maximum, followed by a subsequent decrease in response to the approaching concave portion of the step. The increased discharge above base rate was termed a "burst" and the subsequent absence of response a "pause." The pause was associated with a gap between the step and the skin for the steep, but not the gradual, steps. When the flat, lower side of the step reached the most sensitive spot ("d," Fig. 4), another burst occurred (the "right burst") that was much weaker than the first (the "left burst"). This was followed by a resumption of the basal discharge, which continued until the end of the stroke ("e," Fig. 4).

When the step began moving in the opposite direction, i.e., from the low to the high side of the step, a short, transient response to stretch was followed by a basal level of discharge (locations "e–d," Fig. 4), which ceased altogether (the "right pause") when the concave portion of the step reached the most sensitive spot on the receptive field. This was followed by a burst of impulses (of greater frequency than that generated in the opposite direction) in response to the convex, high side of the step ("b," Fig. 4). A second pause (the "left pause") then occurred when the flat part of the step came into contact with the most sensitive spot, and was followed by a resumption of background discharge, which continued to the end ("a") of the stroke. The neural responses illustrated in Figure 3 suggest how a hypothetical population of identical SAs innervating the skin within the area of contact with a step would be activated if the abscissa represents the loci of different SAs and the ordinate indicates their respective discharge rates at an instant in time.

The relation between the spatial response profile and the location of the most sensitive (von Frey) spot on the receptive field. The most sensitive spot was defined as being at the center of the receptive field mapped by the lowest von Frey filament. The location of this spot on the spatial response profile was that point where the reference mark (located at the sharpest part of each step; see Fig. 1) coincided with the receptive field's center for each stroke. The elapsed time from the beginning of the

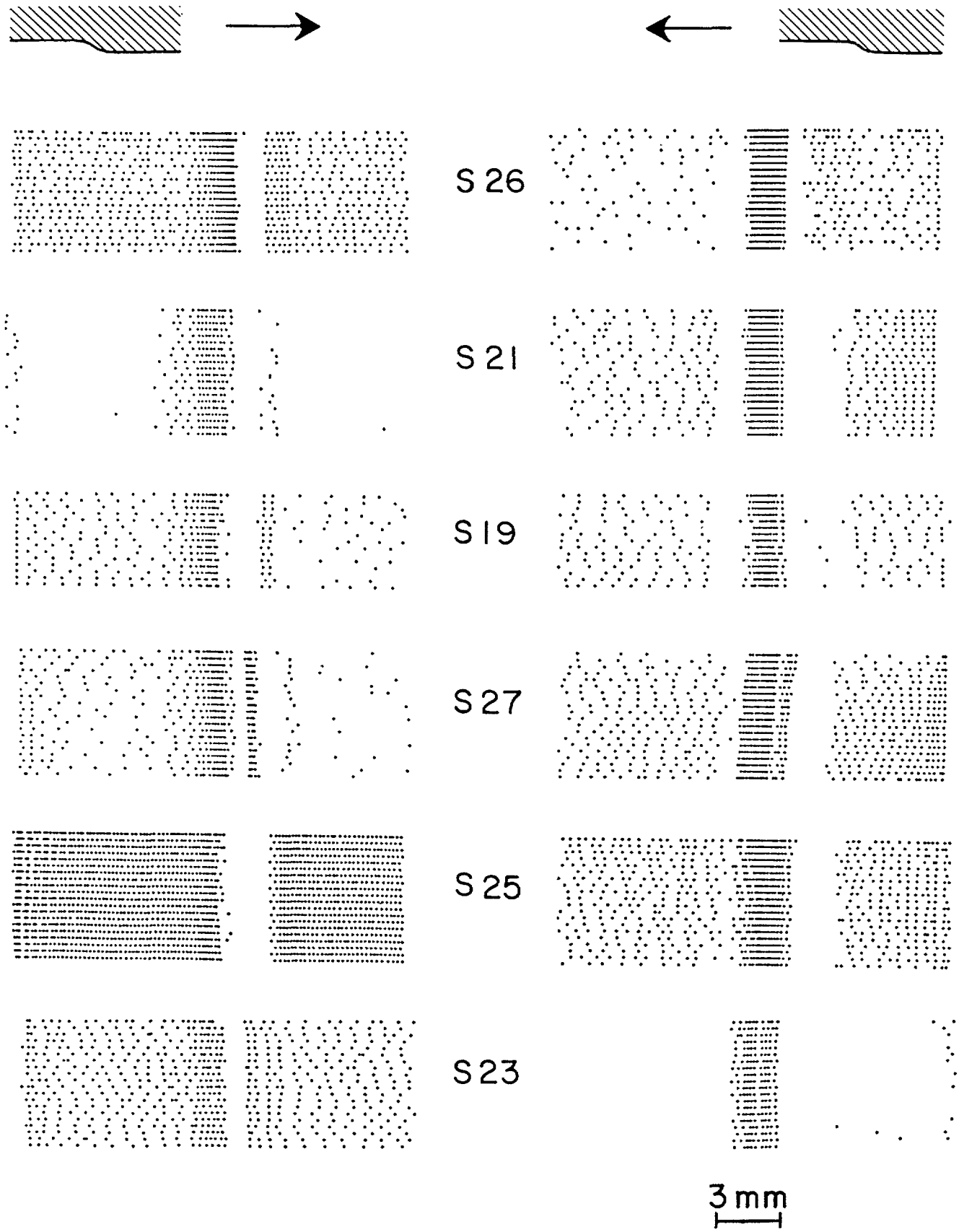

Figure 5. The consistency with which each SA responded to repeated strokes with the same step (*3*) and the variability among responses of different SAs. Each *dot* represents the spatial location of the reference mark on the skin at the occurrence of an action potential and each *row of dots* represents the response during a single stroke in the indicated direction. SA responses are ranked from top to bottom in order of decreasing mean discharge rate during the burst for low-to-high strokes. In each direction, the basal discharge rate is generally less after than before the burst because of adaptation during the stroke.

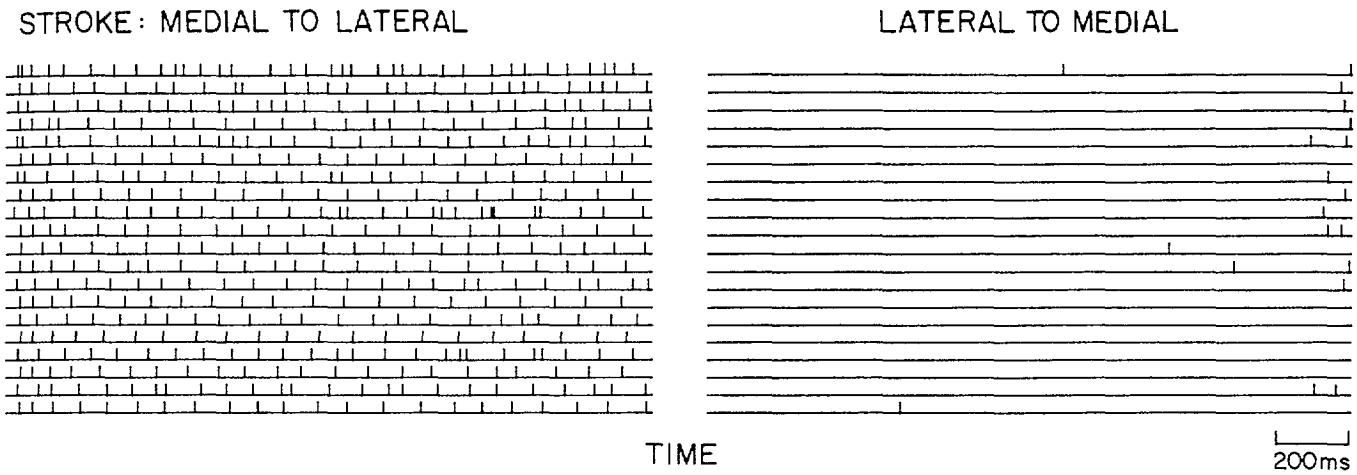

Figure 6. Responses of a "directionally sensitive" SA (S23) to a smooth plate stroked in opposite directions. On each trial, the plate was stroked from a medial to a lateral position across the fingerpad (*left panel*) and then back again (*right panel*) without leaving the skin. There were 20 strokes in each direction. Stroke velocity was 10 mm/sec, stroke distance, 18 mm, and compressional force, 20 gm wt.

stroke to the instant when the reference mark reached the most sensitive spot of the SA's receptive field was obtained from the video data. This elapsed time, when multiplied by the stroke velocity, provided the location of the most sensitive spot on the spatial impulse plot (branched vertical line, Fig. 3).

The mean location of the most sensitive spot coincided with the center of the burst at least to within an accuracy of less than a bin width (0.5 mm). Since the reference mark was on the high side of the step, immediately adjacent to the point of maximum convex curvature, these results indicate that the highest discharge rate on the fiber's spatial response profile for both stroke directions occurred when the sharpest portion of the step was on the point of maximum von Frey sensitivity.

Reproducibility of individual SA responses to repeated presentations of the same step. Although there were considerable differences in the responses of different SAs to the same stimuli, any single SA responded in a highly reproducible manner to repeated presentations of the same step, as illustrated in Figure 5. For some SAs, the discharge rates during the first few strokes were slightly higher than the steady state rates they settled down to, though the pattern of response for a given stroke direction was the same from the first to the last stroke. The variability among different SAs occurred in the values of basal and burst discharge rates, as well as in the widths of bursts and pauses.

Responses to stroking with hand-held steps. Five additional SAs were tested only with hand-held steps that were stroked back and forth across the receptive field along different axes of movement. During such hand-held stimulation, an attempt was made to keep the contact force and stroke velocity as constant as possible. Although nerve impulse counts and movements of the plate were recorded on videotape, no quantitative analyses were carried out. However, it was clear that the patterns of discharge did not differ qualitatively from those evoked during machine-controlled stimulation.

Properties of SA responses that distinguish the direction of movement

There were 2 ways in which almost all SAs' responses to stroking a step from the low to the high side differed from those evoked by stroking in the opposite direction (Fig. 5). First, the pattern of discharge differed. Within the modulatory region, where discharge rate was altered from basal rates, movement from the high to low side (left panels, Fig. 5) elicited a sequence of "burst-pause-burst," while movement from the low to high side (right panels, Fig. 5) produced a sequence of "pause-burst-pause." Second, the peak rate of discharge was almost always greater for movements of the step from low to high, particularly for the steep steps. This was true regardless of any directional preferences in the basal discharge rate (see below). Thus, both a spatial feature (pattern of response) and an intensive feature (discharge rate) differed for the 2 directions of step movement along a given axis.

For the majority of the SAs, there was a third feature, the basal discharge rate, that served to discriminate between directions. Six of the 8 SAs exhibited a preference in basal discharge rate for strokes in 1 of the 2 directions. This bias was not attributable to differences in the amount of lateral skin displacement. In Figure 6, the responses of S23 to a smooth, flat plate stroked in 2 directions along a single axis (perpendicular to the long axis of the finger) are shown. Each stroke from medial to lateral (left panel, Fig. 6) was followed by a stroke in the return direction (right panel, Fig. 6) without the plate being removed from the skin. Virtually identical results were obtained (not shown) if each stroke traveled from lateral to medial and then back from medial to lateral. This particular SA exhibited all the characteristics of an SA Type I, and not Type II; that is, there was no spontaneous activity and no response to remote stretch applied outside of von Frey receptive fields. Also, the borders of the receptive fields were sharply defined (Talbot et al., 1968; Johansson and Vallbo, 1983). Evidence for directional preferences in basal discharge of other SAs is presented in the spatial impulse plots in Figure 5. S21 and S27 exhibited a greater basal rate for strokes in the low-to-high direction, whereas the reverse was true for S7, 23, 25, and 26. S13 and 19 did not distinguish stroke direction by differences in basal rate.

Effect of the shape of a step on SA responses

The responses of an SA (S26) to a steep and a gradual step stroked at 10 mm/sec illustrate the response features affected by changes in step curvature or width (Fig. 7). For movements of the step in either direction, the SA's overall discharge rate during the burst, peak discharge rate, and rate of change in

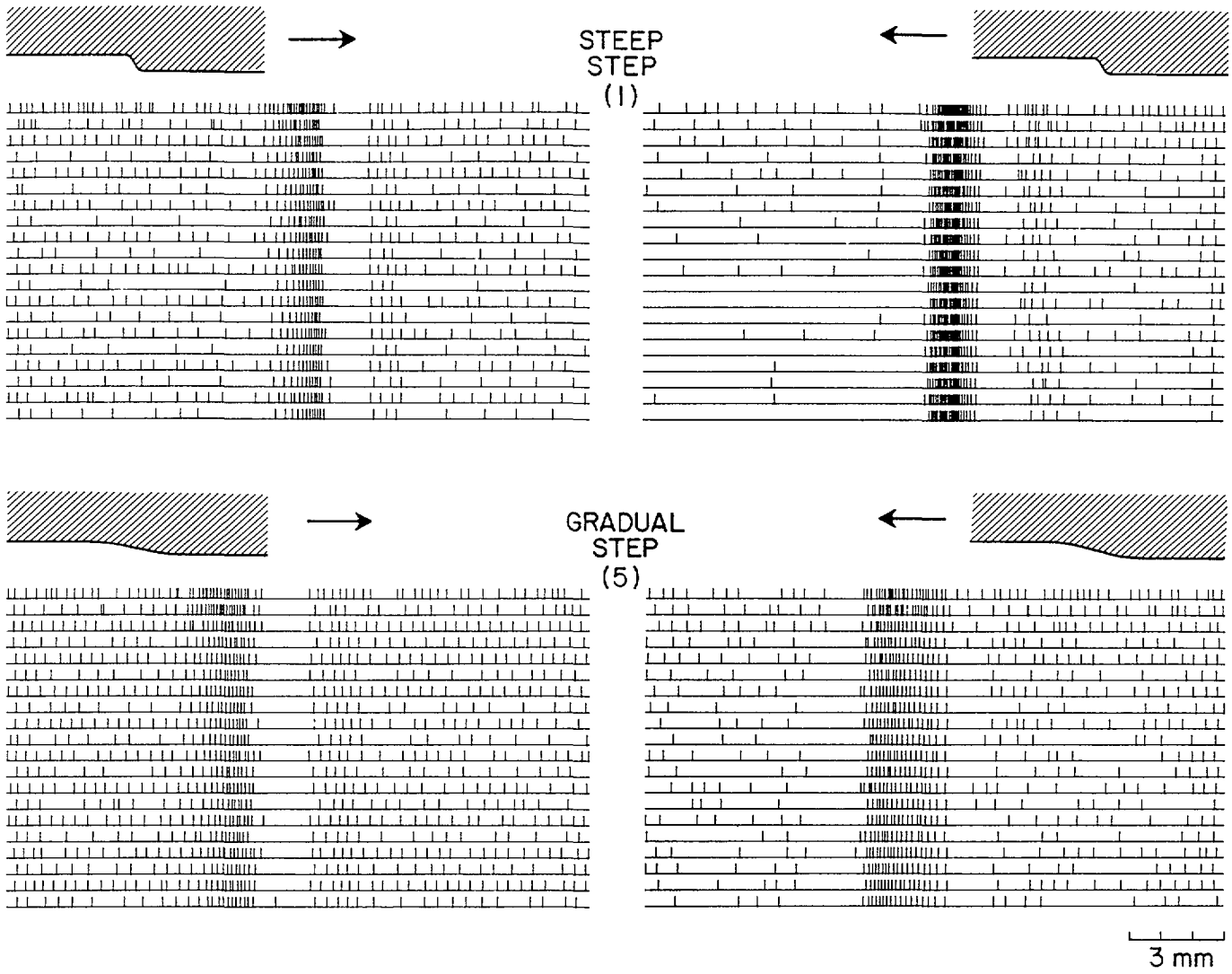

Figure 7. Spatial plots of action potentials evoked in an SA (S26) when a steep and a gradual step were stroked across its receptive field. Steps *1* and *5* were each stroked 20 times from high to low (*left panel*) and from low to high (*right panel*) at a velocity of 10 mm/sec. In each row are the responses to a single stroke in the indicated direction (*arrows*). The impulse plots for step *5* appear shifted to the left with respect to those for step *1*, because the beginnings of the strokes in both plots are aligned and we chose to begin each stroke at a point 9 mm from the center of the step (arrows in Fig. 3) while keeping the total stroke length at 18 mm. For high-to-low strokes, the travel distance between the start position (*a* in Fig. 4) and the point of maximum (convex) curvature (*b* in Fig. 4) is shorter for gradual than for steep steps, resulting in a burst that occurs earlier in time. For low-to-high strokes, the distance between the start position (Fig. 4, *e*) and the beginning of the maximum curvature (Fig. 4, *b*) is longer for gradual than for steep steps and hence the burst starts later in time.

discharge rate between base and peak (and vice versa) during the burst were greater in response to the steep step than to the gradual step. For high to low strokes, the pause width was narrower for steep than for gradual steps, and for low to high strokes, the width of the burst was narrower for the steep step.

Histograms plotting the mean discharge rate (impulses/sec within each bin of 0.5 mm) in response to steps 1 and 5 for strokes in each direction at 10 mm/sec are shown in Figure 8 for 7 SAs. The curve for step 5 in each panel is shifted along the abscissa so that, at a given step position, the reference mark on either of the steps is on the same locus on the skin. The SAs are ranked from top to bottom, from the greatest to the least peak discharge rate during the burst response to step 1, stroked from low to high. This order remained unaltered if the ranking was according to the mean discharge rate during the burst. Thus, it is sufficient to use either of these measures for analyses of step discrimination. The histograms in Figure 8 illustrate how the discharge rate during the burst, or the width of the burst or pause, differed for the steep and the gradual steps.

For quantitative analyses, mean values of burst width, burst discharge rate, and pause width were determined from each SA's response to each step stroked 20 times in each direction at a velocity of 10 mm/sec. Henceforth, for high-to-low strokes, the "burst" refers to the *left* burst and for low-to-high strokes, the "pause" refers to the *right* pause. The remaining burst and pause are not considered further since they were minor features, not consistently altered by changes in shape or stroke velocity. For steps stroking high to low, the left border of the burst was estimated by eye from the alignment of a vertical line along the impulse plots for all strokes (e.g., see Fig. 3*B*). The distance from this line to the last impulse of the burst prior to the pause was measured by the computer and averaged over all strokes

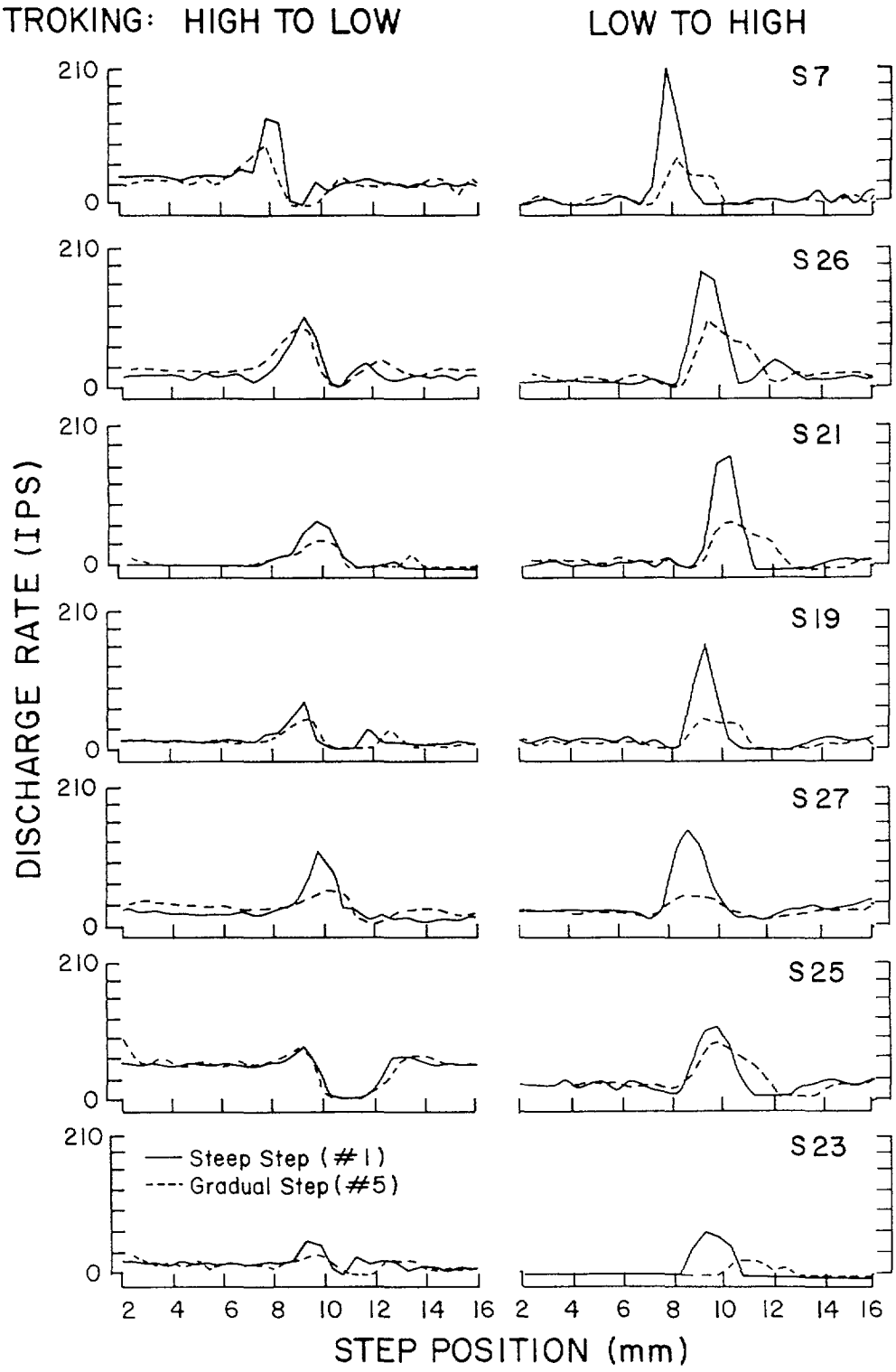

Figure 8. Histograms of mean discharge rate in each SA produced by a steep and a gradual step stroked back and forth. In each panel, the mean discharge rate (impulses/sec or IPS) is plotted for consecutive bins of 0.5 mm. These means were based on the action potentials evoked by each step stroked at 10 mm/sec 20 times in each direction (an exception was S7, for which only 4 strokes were given). Responses to step stroking from high to low (*left column*) and back again from low to high (*right column*) are shown. *Solid and dashed lines* are responses to the steep (*1*) and gradual (*5*) steps, respectively. Histograms for the 2 steps stroked in a given direction have been aligned to the same locus on the skin. Only the responses to the middle 14 mm of the stroke are shown.

(the mean burst width). The mean burst discharge rate was defined as the mean rate during the burst. The mean pause width was the average distance between the right border of the burst and the next impulse to the right. For low-to-high strokes, the width of the pause to the right of the burst was measured and averaged for all strokes. The burst width was determined as the distance between the first impulse of the burst (left border of the right pause) and the last impulse before the left pause in the spatial impulse plots.

The grand means of burst discharge rate (burst rate), burst width, and pause width obtained for all 8 SAs are displayed in Figure 9, along with individual values obtained from a typical SA (S26). In order to determine the significance of these means with changes in the step shape, repeated-measures analyses of variance were performed, followed by pairwise comparisons between individual means, using the Neuman-Keuls procedure (Winer, 1971). The significance level was set at 0.05. Data for step 0 were not included in these analyses or plotted in Figure

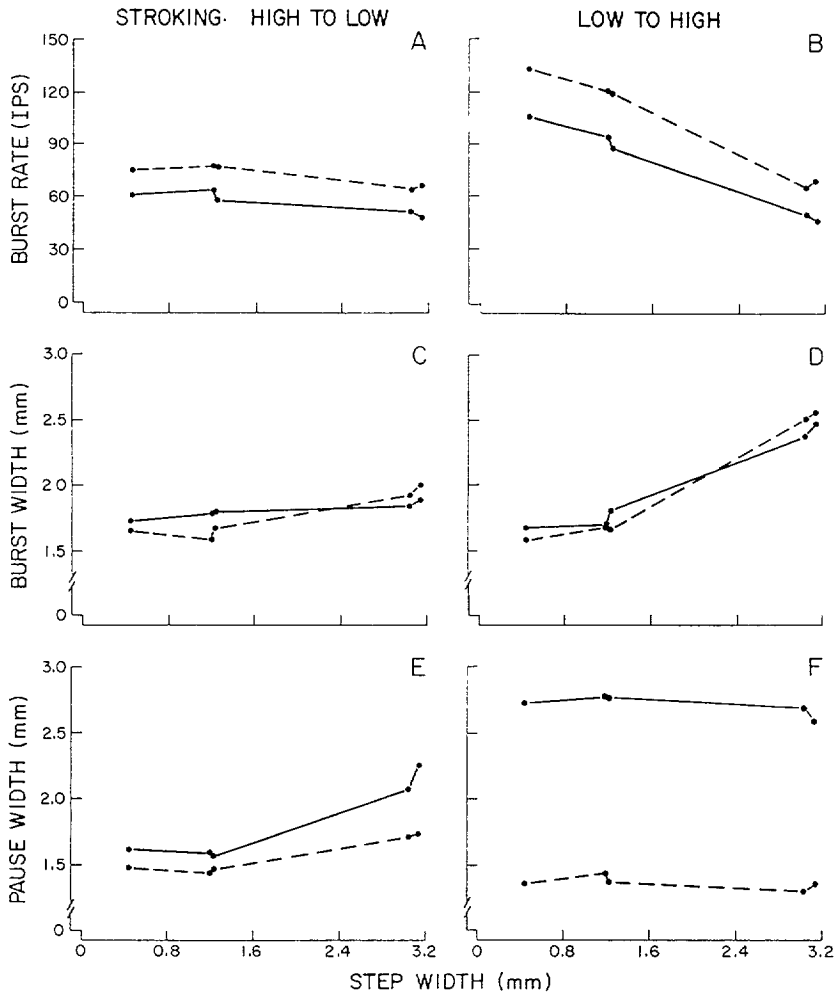

Figure 9. Effects of changes in step shape on certain features of SA responses plotted as functions of step width. In each panel, means are shown for an individual fiber, S26 (*dashed line*), and the grand mean is based on responses of all SAs (*solid line*). *A,B,* Burst rate, i.e., the discharge rate during the burst. *C,D,* The width of the burst. *E,F,* The width of the pause.

9, since the step was used only with 3 of 8 SAs.

When the strokes were from high to low, pause widths (Fig. 9*E*) but not burst widths (Fig. 9*C*) were significantly narrower for steep steps (steps 1–3) than for gradual steps (4 and 5). (Note that the difference of about 0.5 mm in pause widths for steep versus gradual steps is not small; it is a substantial portion of the difference in width between steep and gradual steps, e.g., 1.8 mm between steps 4 and 3 in Fig. 4.) Burst rates for steep steps 1 or 2 (but not 3) were significantly greater than those for the gradual steps. There were no significant differences in any of the 3 measures of responses among steep steps (e.g., 1 versus 2 or 3) or among gradual steps (e.g., 4 versus 5).

When strokes were from low to high, burst rate was significantly greater and burst width significantly narrower for the steep steps than for the gradual steps (Fig. 9,*B,D*). There were no significant changes in pause widths with changes in step widths (Fig. 9*F*). The burst discharge rates were significantly different between steep steps 1 and 3, but not for any other pair of steps within the categories of steep and gradual. Neither of the width measures of response discriminated among steps within the 2 broad categories.

Therefore, the major features of SA responses to steps that provided significant information about differences in step shape were the "spatial" features of pause width (for high-to-low strokes) and burst width (low-to-high strokes) and the "intensive" feature of burst discharge rate (both stroke directions). These features served mainly to distinguish the 2 broad categories of steps, i.e., steep versus gradual. However, finer discriminations among steep steps (only for 1 versus 3) were possible through burst discharge rates for only low-to-high strokes.

Spatial response profile as an indicator of population response. The spatial response profile of an SA (e.g., Fig. 8) can be interpreted as indicating how a population of SAs is activated when a step is stroked across the finger. The pattern of discharge rate provides information about the curvature distribution (along the direction of stroking) on the surface of the step. For example, a rate pattern of steady, burst, pause, and steady corresponds to a surface that is flat, convex, concave, and flat, respectively. For different steps having the same profile of curvature distribution (sinusoidal), discriminative information is provided by SA burst rates and response widths. The width of the burst or pause represents the width of the area on the finger within which SAs are, respectively, maximally activated or silent at a particular instant in time. Different spatial cues are required, depending on the direction of stroking along a given axis. When the step is stroked from low to high, it is the width of the region of skin within which SAs are active (under the sharpest portion of the step) that will be narrower for steep than for gradual steps. Also, within this region, the discharge rate is greater for the steeper step. When the step is stroked from high to low, it is

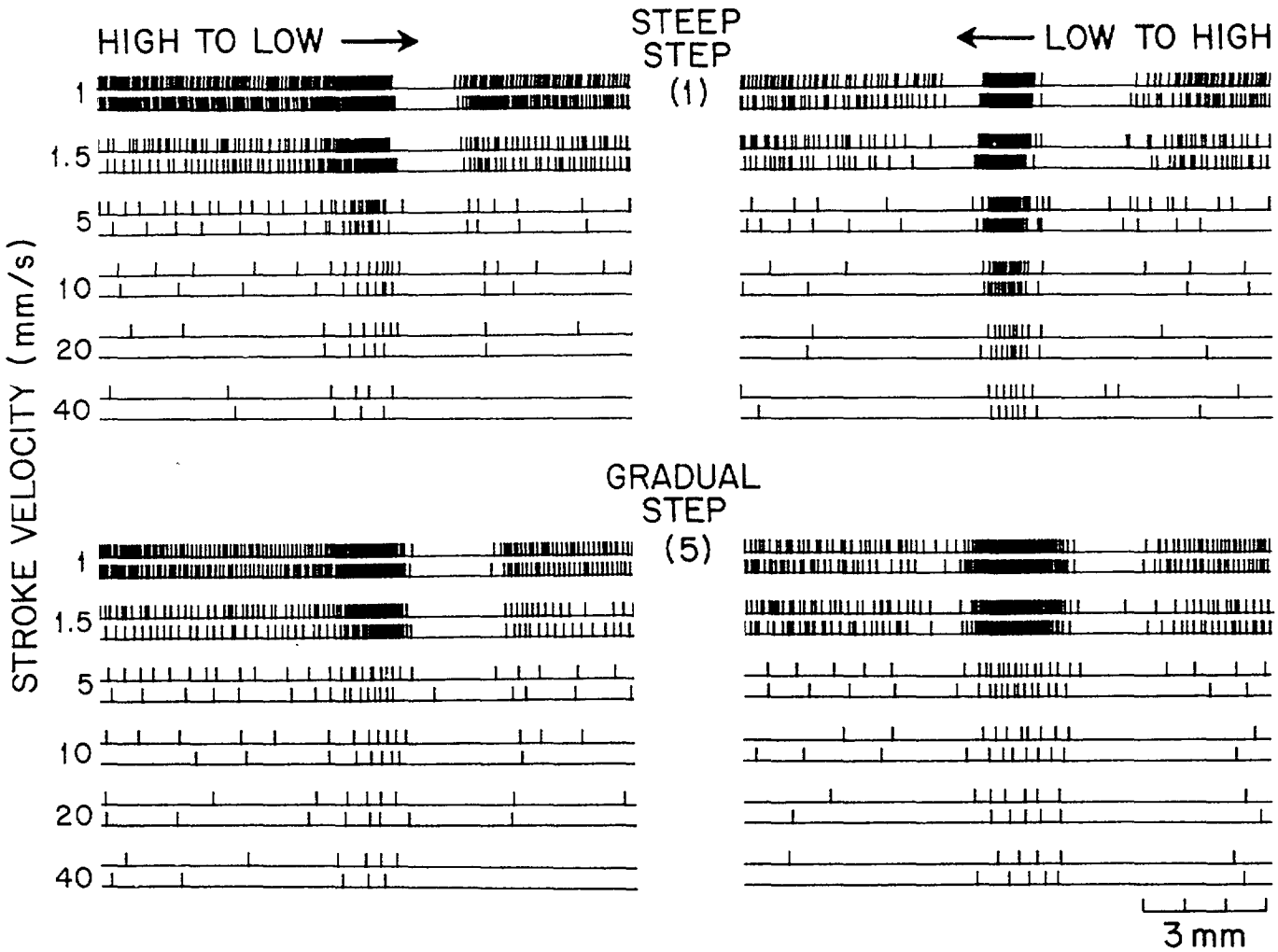

Figure 10. Effects of stroke velocity on the responses of an SA to a steep step and a gradual step. Spatial impulse plots are shown of responses of S19 to steps *1* and *5* stroked 2 times in each direction under 5 different velocities. In order to eliminate small lateral shifts in features of the response due to small differences in the amount of skin stretch (not measured), the responses for each velocity were arbitrarily centered on the middle of the burst, and only responses within 6 mm to either side of the center of the burst are displayed. Note that even though the number of impulses in any spatial interval is greater at lower velocities, the discharge rate is much lower than that at higher velocities, owing to the longer time required to traverse the spatial interval.

the width of region of skin (under the low part of the step transition) within which SAs are silent at an instant of time that changes with step width; the pause width is narrower for steep than for gradual steps, while the widths of skin containing active SAs are the same, although SA discharge rate is greater for steep steps.

Effect of stroke velocity on the responses of SAs to different step shapes

During active stroking of surfaces, the velocity of stroking typically varies considerably. Informal observations of the experimenters during machine-controlled stimulation quickly revealed how easily steps 1 and 5 could be distinguished under a combination of widely different stroke velocities. We therefore investigated how the responses of 8 SAs to different step shapes changed with stroke velocity. Responses of one SA (S19) to steps 1 and 5 are shown in Figure 10 under stroke velocities of 1, 1.5, 5, 10, 20, and 40 mm/sec. These spatial impulse plots have been arbitrarily lined up by centering the bursts. Only the responses extending 6 mm to either side of the center of the burst are displayed. For S19 and other SAs as well, the general pattern of bursts and pauses did not change with stroke velocity. As the velocity was increased, the time required for each stroke decreased (since stroke distance was kept constant at 18 mm), and the number of impulses in a given spatial interval decreased. Nevertheless, discharge rate during the burst increased with velocity. It is also apparent from Figure 10 that, with the exception of strokes at 40 mm/sec for a given step, the width of the pause did not change appreciably with stroke velocity for high-to-low strokes, nor did the width of the burst for strokes from low to high. At a given velocity, both widths were generally narrower for the steep than for the gradual step. The error in estimating response widths is expected to be greater for the higher velocities because of the lesser number of impulses; that is, the "loss" of one impulse, e.g., due to adaptation, would have a greater effect on response width measures for higher velocities than for lower.

The grand means of the mean measurements of rate and width obtained from 7 SAs (20 strokes each) are shown in Figure 11. The "intensive" response measure, mean burst discharge rate,

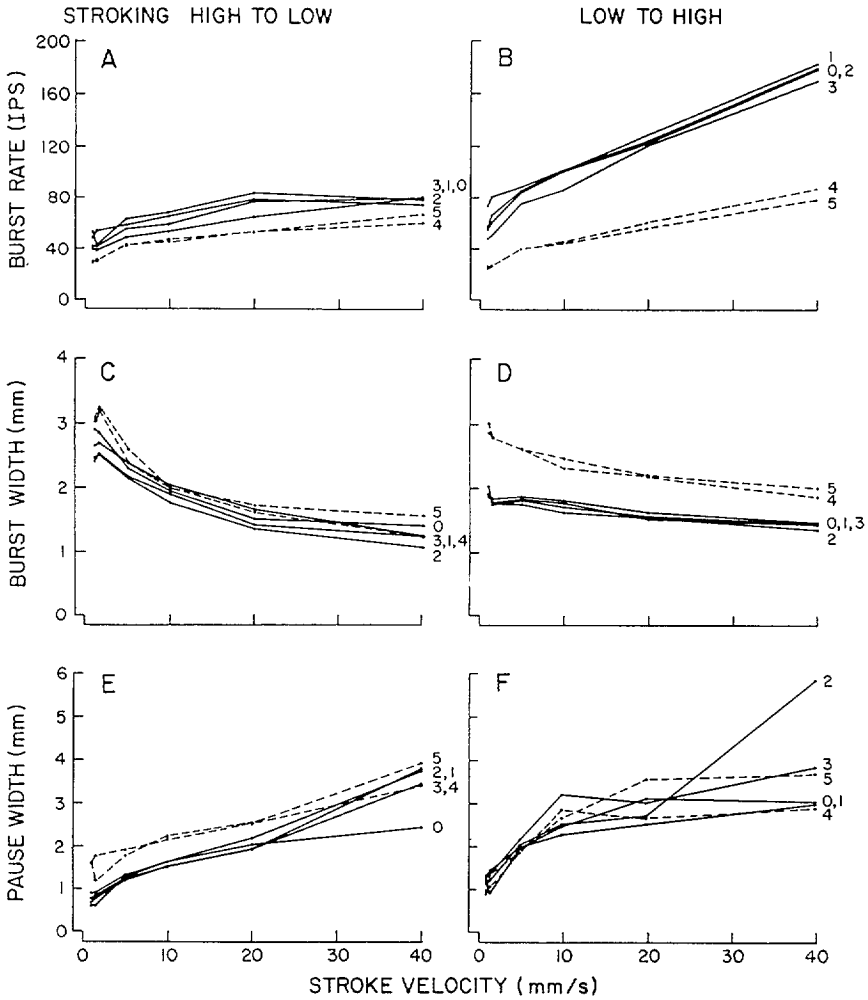

Figure 11. Grand means of the intensive and spatial measures of SA responses to different step shapes as functions of stroke velocity. The intensive measure is the discharge rate during the burst ("burst rate"). The spatial measures are the widths of the bursts and pauses. Responses to gradual steps (*4* and *5*) are *dashed lines*, and responses to steeper steps (*0–3*) *solid lines*. *Data points* are the grand means of the mean responses of 7 SAs (only 3 SAs for step *0*).

as well as the "spatial" features of mean burst width are plotted as functions of stroke velocity. In each panel, response measures for gradual steps (4 and 5) are represented by dashed lines and those for steeper steps (1–3) by solid lines. Analogous curves obtained for individual SAs were very similar to those shown here. Repeated-measures analyses of variance were performed to determine the significance of differences due to stroke direction, step shape, and stroke velocity. The Newman-Keuls procedure was used for pairwise comparisons. The data for step 0 are plotted in Figure 11, but were not included in the statistical analyses, since they were obtained from only 3 of 7 SAs. In the following section, the results of the statistical analyses are summarized separately for the effects of stroke direction, step shape, and stroke velocity on the 3 response measures of burst discharge rate, burst width, and pause width.

Stroke direction. For a given step at any particular stroke velocity, strokes from low to high generated significantly greater burst discharge rates than did strokes from high to low. Otherwise, response measures were comparable for the 2 stroke directions at each stroke velocity (Fig. 11).

Step shape. With the exception of the burst width for high-to-low strokes and the pause width for low-to-high strokes, the response measures were significantly dependent on step shape for both stroke directions. Pairwise comparisons between individual means for a given stroke direction demonstrated that the only consistent significant differences were between the steep steps (1–3) and the gradual steps (4 or 5), and not among steps within either of these categories (for example, 4 versus 5 or 1 versus 2). For strokes from high to low, the burst discharge rate was greater for steep steps 1 or 2 (but not 3) than for gradual steps (Fig. 11*A*). Consistent differences were not obtained between the burst widths of steep versus gradual steps (Fig. 11*C*), while the pause widths of steep steps were narrower than those of gradual steps (Fig. 11*E*). For strokes from low to high, burst discharge rates were greater and burst widths narrower for steep than for gradual steps (Fig. 11,*B,D*), but the pause widths did not differ (Fig. 11*F*).

Stroke velocity. All 3 response measures were significantly dependent on stroke velocity, regardless of stroke direction. As stroke velocity increased, burst discharge rate increased (Fig. 11,*A,B*), the number of impulses in the burst decreased dramatically, the burst width decreased (Fig. 11,*C,D*), and the pause width increased (Fig. 11,*E,F*). There were significant interactions between step shape and stroke velocity for the burst discharge rates only for low-to-high strokes, the differences in rate for steep and gradual steps being greater at the higher stroke velocities. Significant interactions between step shape and stroke velocity were also found for burst widths for both stroke directions, but not for pause widths.

The above results, obtained with 4 strokes at 6 different stroke velocities, are consistent with those obtained with 20 strokes at 10 mm/sec (compare Figs. 9 and 11). The major conclusions as

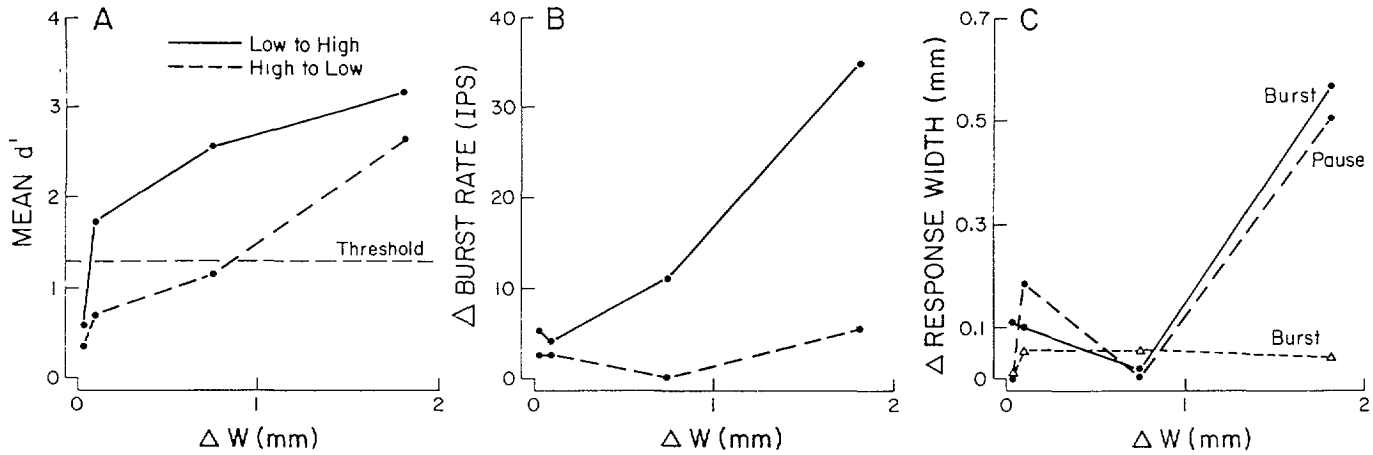

Figure 12. Human sensory discrimination and monkey SA response discrimination of differences in step shapes. The *solid and dashed lines* in each panel represent response measures for step stroking from, respectively, low to high and high to low. Differences in step shapes, represented in terms of differences in step width, ΔW, are plotted in order of increasing magnitude obtained between steps 2 and 3, 4 and 5, 1 and 2, and 3 and 4. *A*, Capacity of humans to detect differences in step pairs. Detection sensitivity (d') was averaged for 5 subjects. *B*, Differences in the mean discharge rate during the burst for each ΔW. *C*, Differences for each ΔW in the mean burst width for stroking in both directions and, in addition, the mean pause width for high-to-low strokes.

to the effects of stroke direction, step shape, and stroke velocity are as follows: (1) Under all stroke velocities, the steep steps (0–3) elicited significantly greater burst discharge rates, narrower burst widths for low-to-high strokes, and narrower pause widths for high-to-low strokes (except at 40 mm/sec) as compared to the gradual steps (4 and 5). Most individual SAs and the mean responses of all SAs for any stroke velocity could not consistently distinguish between steps within the categories of steep or gradual. (2) All response measures changed with stroke velocity. However, there was a range of stroke velocities (between 5 and 20 or 40 mm/sec) within which the above-mentioned response measures for steep steps did not overlap with those for the gradual steps. Within this range, burst discharge rate and burst width for low-to-high strokes or pause width for high-to-low strokes provided unambiguous information about step shape independent of velocity.

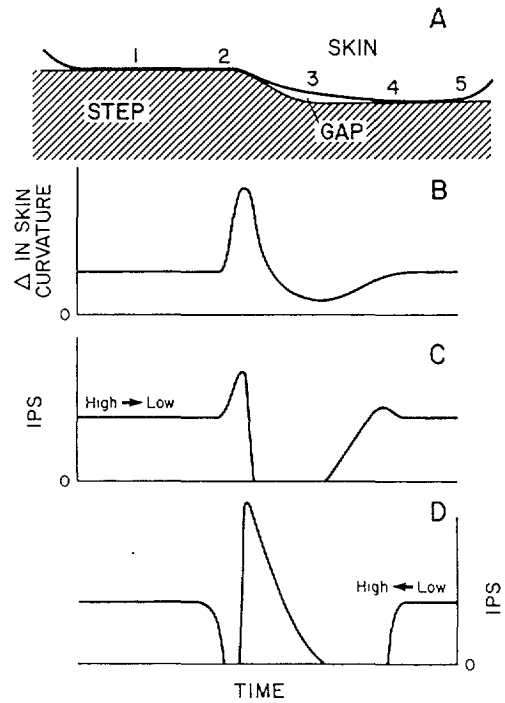

Figure 13. Model of the relationship between changes in skin curvature and SA discharge rate when a finger is actively stroked over a stationary step. *A*, Schematic of the profile of skin deformation against a steep step. The *numbers* refer to certain successive positions of the most sensitive spot within an SA's receptive field as it is moved from the high to the low side of the step (from positions *1* to *5*) or from low to high (positions *5* to *1*). *B*, Schematic of the changes in skin curvature at the most sensitive spot when it reaches each numbered position on the step. *C*, Schematic of the SA's discharge rate as the finger moves from the high to the low side of the step (positions *1–5*). *D*, Schematic of the SA's discharge rate as the finger is moved from the low to high side of the step (positions *5–1*).

Comparison of sensory discrimination performance of humans with SA response discrimination in monkeys

For each of 5 human subjects, a measure of discrimination sensitivity, d', was obtained on the basis of discriminations between the steps in each step pair. The d' values were obtained separately for strokes in each direction. Psychometric functions relating the mean d' (over all subjects) to differences in step width are shown for each stroke direction in Figure 12*A*. These differences (see Fig. 1) from least to greatest were obtained between steps 2 and 3, 4 and 5, 1 and 2, and 3 and 4. The discrimination threshold was defined as a d' of 1.35, which corresponds to 75% correct responses in the absence of response bias. Discriminative measures of mean SA responses to the same differences in step width, delivered under the same stroke velocity of 10 mm/sec, are shown in Figure 12,*B,C*. Each data point is based on group means of the mean responses of 8 SAs. Differences in discharge rate during the burst are plotted in Figure 12*B* for strokes in each direction. Each point was obtained by subtracting the mean rate for the more gradual step in a pair from that evoked by the steeper step. Differences in burst width for strokes in each direction and differences in pause width for high-to-low strokes only are plotted in Figure 12*C*. Mean response widths for the steeper step were subtracted from the mean response widths for the more gradual. The statistical significance of differences in these mean responses was determined by repeated-measures analyses of variance and pairwise

comparisons of individual means, as already described for the data given in Figure 9.

Stroking from low to high. For this stroke direction, all the subjects could discriminate between the shape categories of steep and gradual (i.e., step 3 versus 4). Similarly, there were significant differences in burst discharge rate and burst width in the responses to these 2 steps.

Humans could discriminate between steps within each category. Discrimination was possible between steps 1 and 2 for all subjects, and between steps 4 and 5 for all but one subject. In contrast, differences in SA burst discharge rates or burst widths for these step pairs were not significant. However, it is worth noting that the difference in burst discharge rate for steps 1 and 3 was statistically significant and that all but one SA exhibited a greater rate in response to the steeper step for the step pairs (1 versus 2 and 4 versus 5). Thus, it is possible that with a bigger sample of SAs, differences in burst rate for these step pairs might have reached statistical significance. Lastly, the inability of most subjects (3 of 5 tested) to discriminate between steps 2 and 3, the smallest ΔW, was associated with the absence of any significant differences in discharge rates or burst widths for this stimulus pair.

Stroking from high to low. All human subjects could discriminate steep from gradual (i.e., step 3 from 4), and there was a corresponding large, statistically significant difference in SA pause width, but small and insignificant differences in discharge rate and burst width. However, the discharge rates for steps 1 and 2 were significantly different from those for 4 and 5, and all SAs except one had a higher rate for step 3 than for step 4. Therefore, it is possible that with a bigger sample, the SA discharge rate would discriminate steps 3 and 4. Sensory discriminations between steps within the categories of steep and gradual were not possible for most subjects. Only 2 subjects discriminated between 1 and 2, and none discriminated 2 versus 3 or 4 versus 5. Similarly, there were no significant differences in burst discharge rates or response widths in the SA responses to these stimulus pairs.

The differences in burst discharge rate for each step pair were consistently smaller for high-to-low than for low-to-high stroking. This may have contributed to the poorer sensory discrimination for high-to-low stroking.

Discussion

Combined neurophysiological and psychophysical studies demonstrate that SA mechanoreceptive afferent fibers set the lower limits for tactile spatial resolution (Johnson and Lamb, 1981; Johnson and Phillips, 1981; Phillips and Johnson, 1981a). Also, in response to single bars, edges, and gratings applied vertically to the monkey fingerpad, it was found that SAs, more than RAs, exhibited a greater response to edges than to flat surfaces (Phillips and Johnson, 1981a). This edge-enhancement effect decreased with decreased spacing between the edges of neighboring elements, such as bars in a grating. The spacing, and not the shape of the bars, was varied, and a model was constructed that predicted the SA spatial response profiles to different gratings stepped across the fingerpad. It was concluded that the maximum compressive strain is the relevant stimulus for SAs because it gave the best fit of the SA spatial response profile (Phillips and Johnson, 1981b).

The model proposed by Phillips and Johnson (1981b) could also be used to explain the responses of SAs in the present study to changes in step shape. The step stimuli provided a sequence of curvatures from flat to a right-angled corner. Changes in step curvature and width were accompanied by changes in the discharge rate and spatial features of SA responses. Presumably, with an increase in step curvature, there would be a higher load on the skin in contact with the convex portion of the step, thereby causing a higher compressive strain within the skin at that location. At the present time, however, it is not possible to measure the 4 input variables required for the verification of the model, namely the depth, threshold, and sensitivity of the receptor, and the compressive strain at the receptor. Until these measurements can be made, it may be possible to bypass events at the receptor by modeling the relationship between the shape of the skin deflection profile when an object is applied to the skin (observable input measure) and the responses of mechanoreceptive afferents (observable output measure) (Srinivasan and LaMotte, 1987; M. A. Srinivasan, unpublished observations).

The results of the present study suggest that it is possible to relate the shapes of objects to the responses of SAs using a model that contains parameters that are all empirically verifiable in a direct manner. We hypothesize that SA responses depend not only on the velocity and depth of skin indentation, but also on the rate and the amount of a positive change in skin curvature at the most sensitive spot. A change in curvature is defined as a deviation from the normal convex curvature of the skin surface on the fingerpad. A change toward concavity (as when under an indenting probe) is considered positive, while an increase in convexity is considered negative. The rate of change in curvature (curvature rate) can be either positive or negative, depending on whether the change in curvature is increasing or decreasing with time. During a skin-loading phase, as the amount of curvature change increases, the discharge rate would increase while, for unloading (negative rate of change in curvature), there is minimal or no response. Thus one conceptual "black box" is proposed, with skin curvature change and its rate as inputs, in addition to the displacement and the velocity at the most sensitive spot.

Such a model, while having the disadvantage of not offering an explanation of the actual mechanical stimulus at the level of the receptor, has certain practical advantages. The shape of any object can be represented as a distribution of curvatures. These curvatures could be directly related to the skin deflection profile when the object is applied to the skin (M. A. Srinivasan, unpublished observations). Thus, with the knowledge of object shape, indentation rate, and the mechanical behavior of the skin, calculations of skin curvature change and its rate at the most sensitive spot within the receptive field should be possible; from this, mechanoreceptor responses could be predicted. Eventually, it is hoped, a synthesis of the present approach with that of Phillips and Johnson (1981b) can be achieved with a mechanistic model of the fingertip based on the results of biomechanical experiments, together with independent measurements of receptor depth, threshold, and sensitivity.

Model of SA responses to step stroking

On the basis of the present results and those of previous investigators (e.g., Pubols and Pubols, 1983), we assume, in the following, that the discharge rate of an SA increases both with the amount and velocity of indentation and with the amount and rate of change in the curvature of the skin at the most sensitive spot in the receptive field. Also the SA will respond to a positive rate of change in curvature when a compressive load is applied to the skin, but responds little or not at all to a

negative rate of change in curvature during unloading. Consider, now, that it is the finger that is moved and the step that is stationary; the step is facing upward (Fig. 13*A*) and the contact force of the skin against the step is maintained constant as the finger moves from one end of the step to the other. Consider how the discharge rate evoked in a single SA afferent innervating the fingerpad might be related to changes in skin curvature at the most sensitive spot within the SA's receptive field as this spot is moved across the step (Fig. 13,*B–D*). The following interpretation also applies when the step is stroked across a passive finger.

Finger movement "off the step" (from the high to the low side). If the finger is moved from left to right, i.e., from the high to low side of the step, there is initially a positive change in curvature as the finger is applied to the flat portion of the step (position 1 in Fig. 13*A*). This, together with constant indentation, results in a constant basal discharge rate in the SA (Fig. 13*C*) as skin curvature remains steady (0 rate of change of curvature) when the finger is moved along the flat region. When the most sensitive spot on the receptive field reaches the top edge of the step, the skin curvature at that spot increases (positive curvature rate) to a maximum (2), which evokes a peak discharge rate (within the burst). Next, at the concave portion of the step, the skin tries to return to its initial shape and, for steep steps, a visible gap exists between the skin and the step (3). This "unloading" (negative curvature rate) of curvature, for both steep and gradual steps, results in an immediate cessation of SA responses (the pause). A gradual increase in a positive change in skin curvature follows as the most sensitive spot approaches the bottom, flat portion of the plate (4) (which results in a slight transient increase above basal discharge), whereupon the basal rate is resumed when the skin curvature again becomes steady and indentation depth is maintained (5).

Finger movement "onto the step" (from the low to the high side). Initially, the basal discharge rate is steady (Fig. 13*D*, right side), with a steady change in skin curvature (5 to 4) and depth of indentation. The skin curvature decreases, i.e., increases in the negative direction, when the most sensitive spot in the receptive field approaches the concave portion of a step (4) and SA responses cease (the "right" pause). Then the curvature increases to a maximum (2), resulting in a greater peak discharge rate than the corresponding values resulting from strokes in the opposite direction, owing to (a) a velocity of indentation that was absent during the curvature loading phase for strokes from high to low; (b) a higher rate of change of curvature; and perhaps (c) a greater change in curvature if the skin is pushed into the gap under the steep steps (this "bunching up" of the skin was not taken into account in Fig. 13*B*). This is followed by a pause in discharge (the "left" pause) produced by a brief unloading of curvature, i.e., a negative rate of change in curvature, and a return to basal discharge rate (1).

According to these analyses, for which the curvature profile for both stroke directions is as shown in Figure 13*B*, the following should apply: (1) The flat surfaces on each side of the sinusoidal portion of the step should produce the same changes in skin curvature, and thus the same basal discharge rates (save for slight adaptation effects), for a given stroke direction; (2) the burst discharge should be greater for strokes from low to high than from high to low, especially for steep steps, because of the additional effect of velocity of indentation and a greater rate of change in skin curvature; (3) the burst width for a low-to-high stroke should roughly correspond to the width of the pause produced by a high-to-low stroke; (4) the burst width for a high-to-low stroke should roughly equal the left pause for a low-to-high stroke; (5) the width of the modulatory region should be roughly equal for strokes in either direction; that is, the widths of the left burst plus pause plus right burst for a high-to-low stroke should equal the width of the left pause plus burst plus right pause for a stroke from low to high. These predictions are generally consistent with the data obtained from most SAs (Figs. 5, 8).

The effects of stroke velocity. With increases in stroke velocity, the SA burst discharge rate for a given step increases in either stroke direction because of an increase in the rate of curvature change, and, for low-to-high strokes, an increase in vertical indentation velocity. Also, for both stroke directions, the burst width decreases slightly as stroke velocity is increased, since the passive conformation of the skin around the top edge of the step takes time because of the viscoelastic properties of skin, and because there is less time with increased velocity. Similarly, the width of the response pause will increase with increases in velocity, again because the viscoelastic skin will not conform to the sharpest region of the step as well as it can for slower velocities.

The effects of step shape. For a stroke direction of high to low at a given stroke velocity, changes in step shape from gradual to steep at a given velocity result in a higher burst discharge rate, primarily due to an increase in the amount of skin curvature change, aided by an increased curvature rate (Fig. 11*A*). Since the width of curvature loading, from the initially flat to the sharpest portion of the steps, is approximately the same for both steep and gradual steps, the burst width cannot distinguish these 2 step categories (Fig. 11*C*). The skin stretch (as contrasted with bunching up for strokes from low to high) at the gap under the steep steps aids in creating the differences in the corresponding widths of skin profiles under steep and gradual steps, resulting in a small but significant difference in pause widths (except at 40 mm/sec, Fig. 11*E*).

For strokes from low to high, changes in step shape from gradual to steep at a given velocity cause a higher burst discharge rate owing to increases in the amount of skin curvature change, together with increases in both the vertical velocity of indentation and the rate of change of skin curvature (Fig. 11*B*). These increases are further aided by the bunching up of the skin at the gap under the steep steps. The passive conformation of the skin over the convex portions of the steps is wider for the gradual steps, which have a significantly higher half-cycle wavelength than the steep ones and therefore result in the excellent discrimination of the 2 step categories by burst width (Fig. 11*D*). Since the cessation of response due to the unloading of curvature during the right pause occurs somewhat irregularly, it results in pause widths that do not distinguish consistently between the steep and gradual steps (Fig. 11*F*).

A question raised in the introduction to this paper was whether the responses of cutaneous mechanoreceptors to the shape of an object could be predicted if we knew how the object contacted the skin. We have shown that all of the major features of SA responses to the shapes used can be interpreted as being due to the sensitivity of the SA to the amount and rate of change in skin curvature at its most sensitive spot. Thus, the model relates the shape of the skin deflection profile to the resulting pattern of SA discharge. With the aid of a biomechanical model that

predicts the skin deflection profile under an applied object, together with a mathematical formulation of our model, a prediction of SA responses to the shapes of objects should be possible.

Candidate neural codes for step shape

Differences in discharge rate or response widths (burst or pause) in the mean responses of SAs to steps of different curvature stroked at 10 mm/sec were compared with human capacities to discriminate between these steps. It was found that both burst discharge rate and response widths in SA responses could discriminate between the 2 broad categories of step shape—those that were steep (steps 0–3) and those that were gradual (4 and 5). These categories were easily discriminated by human subjects for strokes in either direction. Further, both sensory discrimination and differences in SA burst discharge rate between steps were greater for strokes from low to high than for strokes from high to low.

Sensory discrimination within each category, that is, between the 2 steepest steps (1 versus 2) and between the 2 gradual steps, was possible for all or most subjects, but only when the steps were stroked from the low side of the step to the high, and not usually for strokes in the opposite direction. The corresponding differences in the discharge rates of SA bursts in response to the steps within each category or to differences in the widths of bursts or pauses were not statistically significant for strokes in either direction, although the differences in discharge rate came close to reaching significance. We hypothesize that the finer sensory discriminations of step curvature among steep steps, or among gradual steps, are probably served by differences in an "intensive" feature of SA responses (burst discharge rate) and not in a "spatial" feature (response width). However, sensory discriminations of grosser differences in curvature (for example, between the categories of steep and gradual) are served by differences in both the spatial and intensive features of SA responses.

It was also found that the intensive and spatial features of SA responses changed not only with the direction of stroking but also with stroke velocity. One might also expect that these features (particularly discharge rate) would change if the overall pressure applied by the step plate against the skin were to be varied. Within a narrow range of velocities of 5–20 or 40 mm/sec, burst discharge rate and burst width for low-to–high strokes, or pause width for high-to-low strokes, provided unambiguous information about step shape independent of velocity. In addition, independent information about the velocity and direction of the movement is available to the brain from afferent input that registers the sequence of events at different spatial loci on the finger as the step is stroked across the skin. Similarly, independent information about the overall contact pressure between the step plate and the skin would be available in the SA's basal discharge rate to the flat portion of the plate. The pattern of SA discharge contains enough information for the brain to be able to extract the shape of an object's surface under a variety of stimulus conditions.

References

Darian-Smith, I., and P. Kenins (1980) Innervation density of mechanoreceptive fibres supplying glabrous skin of the monkey's index finger. J. Physiol. (Lond.) *309:* 147–155.

Darian-Smith, I., and L. E. Oke (1980) Peripheral neural representation of the spatial frequency of a grating moving across the monkey's finger pad. J. Physiol. (Lond.) *309:* 117–133.

Darian-Smith, I., I. Davidson, and K. O. Johnson (1980) Peripheral neural representation of spatial dimensions of a textured surface moving across the monkey's finger pad. J. Physiol. (Lond.) *309:* 135–146.

Johansson, R. S., and A. B. Vallbo (1979) Tactile sensibility in the human hand: Relative and absolute densities of four types of mechanoreceptive units in glabrous skn. J. Physiol. (Lond.) *286:* 283–300.

Johnson, K. O. (1980) Sensory discrimination: Decision process. J. Neurophysiol. *43:* 1771–1792.

Johnson, K. O., and G. D. Lamb (1981) Neural mechanisms of spatial tactile discrimination: Neural patterns evoked by Braille-like dot patterns in the monkey. J. Physiol. (Lond.) *310:* 117–144.

Johnson, K. O., and J. R. Phillips (1981) Tactile spatial resolution. I. Two-point discrimination, gap detection, grating resolution, and letter recognition. J. Neurophysiol. *46:* 1177–1191.

Lamb, G. D. (1983) Tactile discrimination of textured surfaces: Peripheral neural coding in the monkey. J. Physiol. (Lond.) *338:* 567–587.

LaMotte, R. H., and M. A. Srinivasan (1987) Tactile discrimination of shape: Responses of rapidly adapting mechanoreceptive afferents to a step stroked across the monkey fingerpad. J. Neurosci. *7:* 1672–1681.

LaMotte, R. H., G. M. Whitehouse, C. J. Robinson, and F. Davis (1983) A tactile stimulator for controlled movements of textured surfaces across the skin. J. Electrophysiol. Techniques *10:* 1–17.

Phillips, J. R., and K. O. Johnson (1981a) Tactile spatial resolution. II. Neural representation of bars, edges, and gratings in monkey primary afferents. J. Neurophysiol. *46:* 1192–1203.

Phillips, J. R., and K. O. Johnson (1981b) Tactile spatial resolution. III. A continuum mechanics model of skin predicting mechanoreceptor responses to bars, edges, and gratings. J. Neurophysiol. *46:* 1204–1225.

Pubols, B. H., Jr., and L. M. Pubols (1983) Tactile receptor discharge and mechanical properties of glabrous skin. Fed. Proc. *42:* 2528–2535.

Srinivasan, M. A., and R. H. LaMotte (1987) Tactile discrimination of shape: Responses of slowly and rapidly adapting mechanoreceptive afferents to a step indented into the monkey fingerpad. J. Neurosci. *7:* 1682–1697.

Talbot, W. H., I. Darian-Smith, H. H. Kornhuber, and V. B. Mountcastle (1968) The sense of flutter-vibration: Comparison of the human capacity with response patterns of mechanoreceptive afferents from the monkey hand. J. Neurophysiol. *31:* 301–334.

Winer, B. J. (1971) *Statistical Principals in Experimental Design,* McGraw-Hill, New York.